

1 **An update of IPCC climate reference regions for subcontinental analysis of climate model**
2 **data: Definition and aggregated datasets**

3
4 Maialen Iturbide ^a, José Manuel Gutiérrez ^a, Lincoln Muniz Alves ^b, Joaquín Bedia ^c, Ruth
5 Cerezo-Mota ^d, Ezequiel Cimadevilla ^c, Antonio S. Cofiño ^c, Alejandro Di Luca ^e, Sergio
6 Henrique Faria ^{f, f2}, Irina Gorodetskaya ^g, Mathias Hauser ^h, Sixto Herrera ^c, Kevin Hennessy ⁱ,
7 Helene T. Hewitt ^j, Richard G. Jones ^{j, k}, Svitlana Krakovska ^{l, m}, Rodrigo Manzananas ^{n, c}, Daniel
8 Martínez-Castro ^{o, p}, Gemma Teresa Narisma ^q, Intan S. Nurhati ^r, Izidine Pinto ^s, Sonia I.
9 Seneviratne ^h, Bart van den Hurk ^t, and Carolina S. Vera ^u

10 ^a Grupo de Meteorología. Instituto de Física de Cantabria (CSIC-UC). Santander, Spain

11 ^b National Institute for Space Research. Saõ José dos Campos, Brazil

12 ^c Grupo de Meteorología. Dpto. Matemática Aplicada y Ciencias de la Computación. University of
13 Cantabria. Santander, Spain

14 ^d Universidad Nacional Autónoma de México (UNAM). Mexico city, Mexico

15 ^e Climate Change Research Centre and ARC Centre of Excellence for Climate Extremes, University of
16 New South Wales. Sydney, Australia

17 ^f Basque Centre for Climate Change (BC3), Leioa, Spain

18 ^{f2} IKERBASQUE, Basque Foundation for Science, Bilbao, Spain

19 ^g Centre for Environmental and Marine Studies Department of Physics, University of Aveiro. Aveiro,
20 Portugal

21 ^h Institute for Atmospheric and Climate Science, ETH Zurich. Zurich, Switzerland

22 ⁱ CSIRO Oceans and Atmosphere. Canberra, Australia

23 ^j Met Office Hadley Centre. Exeter, United Kingdom

24 ^k School of Geography and Environment, University of Oxford. UK

25 ^l Ukrainian Hydrometeorological Institute. Kyiv, Ukraine

26 ^m State Institution National Antarctic Scientific Center. Kyiv, Ukraine

27 ⁿ Intergovernmental Panel on Climate Change (IPCC), WGI-TSU, Université Paris-Saclay. Paris, France

28 ^o Instituto de Meteorología de Cuba. La Habana, Cuba

29 ^p Instituto Geofísico del Perú. Lima, Perú

30 ^q Manila Observatory, Ateneo de Manila University campus. Quezon City, Philippines

31 ^r Research Center for Oceanography. Indonesian Institute of Sciences. Jakarta, Indonesia

32 ^s Climate System Analysis Group (CSAG), University of Cape Town. South Africa

1 [†]DELTAIRES. Delft, The Netherlands

2 [‡]Departamento de Ciencias de la Atmósfera y los Océanos, FCEyN-UBA. Centro de Investigaciones del
3 Mar y la Atmósfera (CIMA), Instituto Franco Argentino sobre Estudios de Clima y sus Impactos (UMI
4 IFAECI)/CNRS-CONICET. Buenos Aires, Argentina

5

6 **Abstract.** Several sets of reference regions have been used in the literature for the regional synthesis of
7 observed and modelled climate and climate change information. A popular example is the set of reference
8 regions introduced in the Intergovernmental Panel on Climate Change (IPCC) Special Report on
9 Managing the Risks of Extreme Events and Disasters to Advance Climate Adaptation (SREX). The
10 SREX regions were slightly modified for the 5th Assessment Report of the IPCC and used for reporting
11 sub-continental observed and projected changes over a reduced number (33) of climatologically
12 consistent regions encompassing a representative number of grid boxes. These regions are intended to
13 allow analysis of atmospheric data over broad land or ocean regions and have been used as the basis for
14 several popular spatially-aggregated datasets, such as the seasonal mean temperature and precipitation in
15 IPCC regions for CMIP5.

16 We present an updated version of the reference regions for the analysis of new observed and simulated
17 datasets (including CMIP6) which offer an opportunity for refinement due to the higher atmospheric
18 model resolution. As a result, the number of land and ocean regions is increased to 46 and 14
19 respectively, better representing consistent regional climate features. The paper describes the rationale for
20 the definition of the new regions and analyses their homogeneity. The regions are defined as polygons
21 and are provided as coordinates and shapefile together with companion R and Python notebooks to
22 illustrate their use in practical problems (e.g. calculating regional averages). We also describe the
23 generation of a new dataset with monthly temperature and precipitation, spatially aggregated in the new
24 regions, currently for CMIP5 and CMIP6, to be extended to other datasets in the future (including
25 observations). The use of these reference regions, dataset and code is illustrated through a worked
26 example using scatter plots to offer guidance on the likely range of future climate change at the scale of
27 the reference regions. The regions, datasets and code (R and Python notebooks) are freely available at the
28 ATLAS GitHub repository; <https://github.com/SantanderMetGroup/ATLAS>,
29 doi:10.5281/zenodo.3968318 (Iturbide et al., 2020).

30 **KEY WORDS:** *Regional climate change; Climatic regions; CMIP5; CMIP6; Climate change projections;*
31 *Reproducibility*

32 *Copyright statement. The reference regions and the aggregated datasets derived from CMIP5 described in this paper*
33 *are made available in the ATLAS GitHub repository (<https://github.com/SantanderMetGroup/ATLAS>) under the*
34 *Creative Commons Attribution (CC-BY) 4.0 license, whereas the scripts and code are made available under the GNU*
35 *General Public License (GPL) v3.0. Additional products included in the ATLAS GitHub comply with the licenses of*
36 *the original datasets and are periodically updated (e.g. CMIP6 aggregated dataset).*

37 **1 Introduction**

38 Different sets of climate reference regions have been proposed in the literature for the regional synthesis of observed
39 and model-projected climate change information, and have been subsequently used in the different Assessment
40 Reports of the IPCC. The Giorgi reference regions (originally 23 squared regions proposed in Giorgi and Francisco,
41 2000) were used in the third (AR3, Giorgi et al., 2001) and fourth (AR4, Christensen et al., 2007) IPCC Assessment
42 reports. These regions were modified using more flexible polygons in the IPCC SREX special report (Seneviratne et
43 al., 2012) and then slightly modified and extended to 33 regions (by including island states, the Arctic and
44 Antarctica) for the fifth Assessment Report (AR5, van Oldenborgh et al., 2013), as shown in Figure 1a. The objective
45 in these revisions was to improve the climatic consistency of the regions so they represent sub-continental areas of
46 greater climatic coherency. This process typically resulted in a larger number of smaller regions, constrained by the
47 relatively coarse resolution of the global models, since each region should encompass a sufficient number of
48 gridboxes. The IPCC AR5 reference regions (http://www.ipcc-data.org/guidelines/pages/ar5_regions.html; last
49 access: 30 July 2020) were developed for reporting sub-continental CMIP5 projections (with an average horizontal

1 resolution greater than 2°) and were quickly adopted by the research community as a basis for regional analysis in a
2 variety of applications (Barring and Strandberg, 2018; Madakumbura et al., 2019). Moreover, these regions have
3 been used to generate popular spatially aggregated datasets, such as the *seasonal mean temperature and precipitation*
4 *in IPCC regions for CMIP5* (McSweeney et al., 2015), which provides ready-to-use information from the CMIP5
5 models, suitable for regional analysis of climate projections and their uncertainties. This dataset can be directly used
6 by researchers and stakeholders for a variety of purposes, including assessing the internal variability, model and
7 scenario uncertainty components (Hawkins and Sutton, 2009), or assisting in the comparison and selection of
8 representative sub-ensembles for impact studies (e.g., Ruane and McDerimid, 2017).

9 The increasing availability of CMIP6 multi-model simulations (O'Neill et al., 2016; NCC editorial, 2019) offers an
10 opportunity to refine the AR5 reference regions—due to the higher atmospheric model resolution, typically around
11 1°—and also to produce ready-to-use aggregated regional information for the updated reference regions. This is a
12 timely task due to the great interest of the research community in the higher sensitivity of some CMIP6 models and
13 the potential implications for climate change studies (Forster et al., 2020). Here, we present the results of an initiative
14 carried out during the last year to achieve this goal. First, we present the updated regions (referred to as updated IPCC
15 WGI reference regions) and describe the rationale for the revision, which was guided by two basic principles: 1)
16 climatic consistency and better representation of regional climate features and 2) representativeness of model results
17 (sufficient number of model gridboxes per region). Climatic homogeneity is characterized in terms of mean
18 temperature and precipitation considering Köppen-Geiger climatic regions (Rubel and Kottek, 2010), the annual
19 cycle and projected changes of the reference regions. The resulting 46 land plus 14 ocean regions (see Figure 1b) are
20 provided as coordinates (in csv format and as shapefile) with companion notebooks to illustrate their use in R and
21 Python.

22 Second, we describe the monthly regional temperature and precipitation dataset obtained by spatially aggregating the
23 model data over the reference regions (currently for CMIP5 and CMIP6, to be extended later to observations and
24 additional datasets). Finally, the use of these reference regions, datasets and code is illustrated through a reproducible
25 example which analyses the likely range of future temperature and precipitation changes that are expected for
26 different European regions using scatter plots.

27 Section 2 presents the data and methods used in this work. Sec. 3 describes the reference regions and their rationale.
28 The regionally aggregated CMIP5 dataset is presented in Section 4 and links are provided for additional aggregated
29 datasets (e.g. CMIP6, which are periodically updated); a reproducible illustrative example is described in Sec. 5.
30 Finally, conclusions and discussion are presented in Sec. 6.

31 **2 Data and Methods**

32 We use global gridded observations to characterize the regional climatological conditions at a sub-continental scale.
33 In particular, we use CRU TS (version 4.03; Harris et al., 2014; Harris and Jones, 2020) providing monthly
34 precipitation and temperature with a resolution of 0.5° over land for the period 1901-2017. Figure 2a-b shows the
35 annual mean temperature and precipitation climatology for the period 1981-2010. CRU TS does not cover Antarctica,
36 which is therefore infilled with an alternative dataset, namely the EWEMBI gridded observations (Lange, 2019).
37 Figure 2c shows the Köppen-Geiger climatic regions (Rubel and Kottek, 2010) computed from these datasets.
38 Quantifying the observational uncertainty is an increasing concern in climate studies, particularly for precipitation
39 (Kotlarski et al., 2019). Therefore, we use two additional observational datasets for precipitation in some parts of this
40 study: 1) Global Precipitation Climatology Centre (GPCC, v2018 used here; Schneider et al., 2011) providing
41 monthly land precipitation values with 0.5° resolution for the period from 1891 to 2016, and 2) Global Precipitation
42 Climatology Project (GPCP; Monthly Version 2.3 gridded, merged satellite/gauge precipitation; Huffman et al.,
43 2009), providing monthly land and ocean precipitation values with a resolution of 2.5° for the period 1979-2018. We
44 show results for the current WMO climatological standard normal period 1981–2010 (WMO, 2017).

45 Global model scenario data was downloaded for CMIP5 (Taylor et al., 2012)/CMIP6 (O'Neill et al., 2016) models
46 for the historical (1850- 2005/1850-2014) and RCP2.6/SSP1-2.6, RCP4.5/SSP2-4.5 and RCP8.5/SSP5-8.5 future
47 scenarios (2006-2100/2015-2100). Data for CMIP5 (curated version used for IPCC-AR5) was downloaded from the
48 IPCC Data Distribution Center (https://www.ipcc-data.org/sim/gcm_monthly/AR5/index.html; last accessed, 31 Dec
49 2019) and for CMIP6 was downloaded from the Earth System Grid Federation (ESGF, Balaji et al., 2018); a
50 periodically updated inventory is available at the ATLAS GitHub repository (in the *AtlasHub-inventory* folder). All
51 model data has been interpolated to common 2° (for CMIP5) and 1° (CMIP6) grids—separately for land and ocean
52 gridboxes using conservative remapping (using CDO with the models and target land/sea masks; CDO, 2019),—
53 which are typical model resolutions for CMIP5 and CMIP6 models, respectively. The common grids and land/sea
54 masks are available in the ATLAS GitHub repository (in the *reference-grids* folder).

1 In this paper we illustrate the results using the curated CMIP5 dataset and refer to the ATLAS GitHub repository for
2 similar results for CMIP6. Figure 2d-e shows the CMIP5 multi-model climate change signal for annual mean
3 temperature (in absolute terms) and precipitation (relative, in %) for RCP8.5 2081-2100 (w.r.t. the modern climate
4 baseline 1986-2005 used in AR5). This figure shows the typical spatial climate change patterns and is used to
5 illustrate the consistency of the regional signals in the climate reference regions.

6 **3 Reference Regions: Rationale and Definition**

7 The Giorgi reference regions were originally defined with the goal to represent consistent climatic regimes and
8 physiographic settings, while maintaining an appropriate size for model representation (thousands of kilometers, to
9 contain several model gridboxes), using some subjectivity in the final selection (Giorgi and Francisco, 2000). Here,
10 we are guided by the same basic principles to define the revised reference regions (see Figure 1b). Climatic
11 homogeneity is characterized in terms of mean temperature and precipitation considering Köppen-Geiger climatic
12 regions (see Figure 2) and also the annual precipitation cycle (Figures 3 and 4); in the later case, observational
13 uncertainty is analysed using the three alternative datasets described in Sec. 2. Representativity of model results
14 (sufficient number of gridboxes per region) is analysed at the end of this section in Figure 5.

15 **3.1 Definition of new regions**

16 In North America, the Polar Greenland-Iceland (GIC) region was divided in two, Northeastern North America (NEN)
17 and Greenland/Iceland (GIC), to better accommodate the subarctic and Polar climates, respectively (Figure 2c). The
18 eastern and central Northern America regions (ENA and CNA) are maintained mostly unaltered while the western
19 part was reorganized to increase climate consistency. The new Northwestern region (NWN) includes mostly the
20 subarctic regions, the modified western region (WNA) encompasses a variety of regional intermixed climates
21 (semiarid, Mediterranean, and continental) which are difficult to further separate due to the complex orography, and
22 the new North Central America (NCA) region includes the semiarid and arid climates of Northern Mexico, separating
23 them from the tropical climates in southern Central America which constitute a new region (SCA). The Caribbean
24 (CAR) region has been modified to fully include the Greater Antilles.

25 In South America, the old northwestern Amazonia region is divided into three subregions to separate the Northern
26 South America (NSA) region from the western region (NWS) —which includes the northern Andes Mountains range,
27 — and the South America Monsoon (SAM) region. These regions represent sub-continental areas of greater climatic
28 coherency (Espinoza et al 2019), both in terms of climate and climate change signals (Figures 2c-e), and exhibit
29 characteristic seasonal precipitation cycles (Figure 3), with a rainy season from October to March in SAM and no
30 clear wet and dry seasons for NSA and NWS. The Northeastern region is maintained, but the name is changed to
31 Northeastern South America (NES). The old southern South America region is divided in two, separating the
32 northern (southeastern South America, SES) and southern (SAS) parts, the later encompassing the mostly cold desert
33 climates exhibited in this region (see Figure 2c).

34 The three European reference regions NEU, CEU (renamed Western and Central Europe, WCE) and MED have been
35 maintained unaltered since they encompass the main regional climates in Europe, from subarctic, to
36 oceanic/continental and to Mediterranean. However, an additional region has been introduced in Eastern Europe
37 (EEU), encompassing the continental climate on the western side of the Ural mountain range.

38 For Africa, the old WAF region has been divided in divided in two (WAF and CAF, see Figure 2b); although these
39 regions have similar Köppen-Geiger climates (see Figure 2c), they have very different annual cycles (Figure 4) and
40 therefore should be analysed independently (Diedhiou et al., 2018). A similar situation was found in the original EAF
41 (Osima et al., 2018) which was also divided in two, a Northern subregion (NEAF) which includes the arid region of
42 the Horn of Africa, and a Southern subregion (SEAF). These two regions also exhibit different precipitation seasonal
43 cycles, with different timing of the annual maximum (see Figure 4). Moreover, the South Africa region SAF was also
44 divided in two subregions with different rainfall regimes (Maure et al., 2018), the western subregion (WSAF)
45 including the arid regional climates, and the Eastern region (ESAF).

46 In the case of Asia, Northern Asia is subdivided in a Northern subarctic region (RAR), two regions for Western
47 (WSB) and Eastern (ESB) Siberia and a region for the Russian far East (RFE). The original Western Asia region
48 (WAS) is divided in two regions, Western central Asia (WCA) and the Arabian Peninsula (ARP), the later with an
49 arid climate; these two sub-regions exhibit a distinct seasonal cycle (see Figure 4). The old Tibetan plateau (TIB)
50 region is divided in two subregions, separating the highland climate of the Tibetan plateau in the South (TIB) from
51 the northern arid subregion (Eastern Central Asia, ECA). The South Asia (SAS), East Asia (EAS) and Southeast Asia
52 (SEA) are maintained unaltered (with the exception of adjustments caused by changes in neighboring regions).

1 Regarding Australasia, the Southern region (SAU) is now further south (better differentiating the rainfall climatology,
2 Fig. 2c) and separated from the oceanic New Zealand (NZ). The Northern region is divided in three subregions to
3 increase climatic consistency (CSIRO, 2015; see Figure 1b) separating the northern tropical region (NAU), the
4 central arid region (CAU) and the subtropical east coast (EAU).

5 In contrast to the AR5 regions, those defined in this paper also include 14 oceanic regions (note that the Caribbean
6 and Mediterranean and considered both land and ocean regions, defined considering the land and sea masks,
7 respectively). Since these largely exclude the coastal zones (which are often included in the “land” regions), they are
8 generally more suitable for the analysis of large-scale atmospheric data. Figure 2d and e demonstrates that in this
9 respect the ocean regions are a good addition to the AR5 definitions even though they were not developed with the
10 intention of defining ocean basin masks for zonal means used by oceanographers. However, we note that since the
11 coastal regions can be defined by applying a land-sea mask to the land boxes, it is possible to combine regions to
12 enable the more traditional ocean basin definitions used by oceanographers to be produced to a large extent (albeit
13 not exactly).

14 3.2 Representativeness of model results

15 The higher atmospheric resolution of CMIP6 yields better model representation on the reference regions (more
16 gridboxes per region) allowing a revision for better climatic consistency (e.g. dividing heterogeneous regions) while
17 preserving model representativeness. Figure 5 illustrates this, displaying the number of gridboxes (only land
18 gridboxes for land regions) in each of the AR5 (last column) and revised (first column) reference regions for the two
19 reference grids (1° and 2°), as well as for the CMIP6 model grids (representing the multi-model mean of gridbox
20 numbers). This figure shows that the 1° grid provides a good reference for CMIP6. Moreover, it shows that the new
21 reference regions are more representative than the AR5 ones due to the increase of model resolution (see Figures 5a
22 and 5d, corresponding to the cases of CMIP6 data on the updated reference regions, and to CMIP5 data in the original
23 AR5 regions, respectively). The regions with the smallest number of gridboxes correspond to three island regions:
24 The Caribbean (CAR), New Zealand (NZ), and Madagascar (MDG), with around 20-60 gridboxes per region. Note
25 that the updated regions are also suitable for the analysis of CMIP5 data (at 2° resolution, Fig. 5c) since all regions
26 encompass over ten land gridboxes, with the exception of the three above-mentioned regions, where results should be
27 interpreted with caution.

28 These updated regions are defined as polygons (the lines in Figure 1 are straight lines on a projected plane) and are
29 provided as coordinates and shapefile at the ATLAS GitHub (*reference-regions* folder); the reference grids and land-
30 sea masks can be found at the *reference-grids* folder. Moreover, companion R and Python notebooks are also
31 available (*reference-regions/notebooks*) to illustrate their use in practical problems (e.g. calculating regional
32 averages).

33 4 Regionally Aggregated CMIP Datasets

34 The seasonal mean temperature and precipitation in IPCC regions for CMIP5 McSweeney et al. (2015) is a popular
35 dataset based on the IPCC AR5 reference regions, suitable for the regional analysis of climate projections and their
36 uncertainties. Here we extended this idea to the new regions and model data and computed aggregated monthly
37 results over the different reference regions (see Figure 1b) for all the CMIP5 model runs (and also the available
38 CMIP6 ones), considering land only, sea only, and land-sea gridboxes (the land/sea masks are available in the
39 ATLAS GitHub repository, *reference-grids*). Results are calculated for each model run and stored individually as a
40 text-csv file, with regions in columns (including the global results in the last column) and dates (months) in rows;
41 results for a single run are included directly in the ATLAS Github repository (*aggregated-datasets* folder), and links
42 are provided to the general dataset (full ensemble with all runs) which allows for internal variability studies.

43 Whereas the aggregated CMIP5 dataset is final, results for CMIP6 will be regularly updated when new data becomes
44 available at ESGF; these two datasets constitute alternative lines of evidence for climate change studies and the
45 ATLAS initiative presented here allows facilitates intercomparison of results and consistency checks for the reference
46 climatic regions. Note that although the aggregated data provides summary climate information for each sub-
47 continental region which is useful for a broad spectrum of users, detailed climate information at local or regional
48 scales (in each sub-continental region) would be required for further regional analysis.

49 5 Illustrative Case Study

50 To demonstrate a potential application of the reference regions and the associated regionally-averaged CMIP data
51 (for temperature and precipitation), we show a simple case study illustrating the projected range of future

1 temperature/precipitation change. This can provide useful context information for a variety of impact and adaptation
2 studies. In particular, we use scatter plots to show the median, 10th, and 90th percentiles of the CMIP5 ensemble
3 change. We focus on three illustrative European regions (NEU, WCE and MED) with opposite climate change
4 signals for precipitation (see Figure 2e). The code and data needed to run this example (which can be extended to
5 other regions, or combination of regions, and datasets, e.g. CMIP6) are all available at the ATLAS GitHub repository
6 (*aggregated-datasets/scripts* folder) and can be run in a local R session accessing the GitHub data with no further
7 requirements.

8 Figure 6 shows the projected changes in annual mean temperature and precipitation resulting from the script
9 *scatterplots_TvsP.R*. In particular, results from RCP2.6, RCP4.5 and RCP8.5 scenarios for early (2021-2040), mid
10 (2041-2060 and 2061-2080) and late (2081-2100) 21st century — relative to the 1986-2005 baseline period — for
11 each of the three European subregions are displayed. This figure evidences an increase of temperature in all
12 European domains —with similar warming in all regions for the different scenarios and future periods— and a
13 consistent meridional gradient of changes in precipitation, with a clear precipitation increase in NEU, non-changing
14 conditions in WCE (uncertainty range crossing the zero line), and reduced precipitation over MED. The same scripts
15 can be applied to the currently available CMIP6 dataset by changing two parameters to check the consistency of these
16 results for the updated models and scenarios.

17 Note that this illustrative example can be modified to serve different purposes. For instance, the same diagram can be
18 adapted to display the individual model values (or to select the subset of models spanning the uncertainty range) in
19 order to assist in the comparison and the selection of representative sub-ensembles for impact studies (e.g. Ruane and
20 McDermid, 2017). The calculation of the regional aggregated values is time consuming (computed offline and results
21 are provided in the GitHub repository); however, accessing the values and plotting the results is straightforward and
22 the scripts provided run in a few seconds.

23 6 Conclusions and Discussion

24 A new set of 46 land plus 14 ocean regions is introduced in this work updating the previous set of IPCC AR5-WGI
25 reference regions for the regional synthesis of model-projected climate change information (in particular for the new
26 CMIP6 simulations). The new regions increase the climatic consistency of the previous ones —by rearranging and
27 dividing regions exhibiting mixed regional climates— and have a suitable model representation (the minimum is in
28 the range 20-60 model gridboxes for three particular island regions: the Caribbean, New Zealand and Madagascar.
29 This revision was guided by the basic principles of climatic consistency and model representativeness, but there is of
30 course some subjectivity in the final selection.

31 We also present a new dataset of monthly CMIP5/6 spatially aggregated information using the new reference regions
32 and the available CMIP5 (from the IPCC-DDC) and CMIP6 data (from ESGF, as of 30 September 2019), and
33 describe a worked-out example on how to use this dataset to inform regional climate change studies, in particular
34 about the likely range of future temperature/precipitation changes for the different European reference regions using
35 scatter plots.

36 7 Code and data availability

37 The present work is part of the climate change ATLAS initiative (which is aligned with IPCC AR6 activities). The
38 definition of the regions, the code and the associated spatially-aggregated datasets are available at the GitHub
39 ATLAS repository: <https://github.com/SantanderMetGroup/ATLAS>, doi:10.5281/zenodo.3968318 (Iturbide et al.,
40 2020). The ATLAS project builds in the publicly available climate4R R framework (Iturbide et al., 2019) (available
41 under the GNU General Public License v3.0) and provides additional functions which may be relevant for the users
42 of the reference regions and aggregated datasets, such as the calculation of global warming levels, thus enhancing the
43 functionalities presented in this work. The python notebook is based on the open source projects *regionmask* (Hauser,
44 2019) and *xarray* (Hoyer and Hamman, 2017), among others. The results for CMIP5 are based on the final curated
45 dataset used for IPCC-AR5, but other datasets will be updated periodically when new data becomes available (e.g.
46 CMIP6, still in progress).

47 Regarding the original datasets used in this work, all of them are publicly available from the local providers — CRU
48 TS4.03 is distributed under the Open Database License, and EWEMBI and GPCCv2018 are distributed under the
49 Creative Commons Attribution 4.0 International License — and/or the Earth System Grid Federation (ESGF, Balaji
50 et al., 2018) — CMIP5 and CMIP6. Moreover, for the sake of reproducibility some datasets have been also
51 replicated at the Santander Climate Data Service which is transparently accessible from climate4R via the User Data

1 Gateway (registration is required to accept the terms of use of the original datasets; more information at
2 <http://meteo.unican.es/udg-wiki>, last access: 30 July 2020).

3 **Author contributions.** Gutiérrez J.M. and Iturbide M. conceived the study and wrote the code and the manuscript;
4 vandenHurk B. conceived the case study; Iturbide M. and Hauser M. implemented the R and Python companion
5 notebooks; all authors contributed to the definition of the regions, to the discussion and revised the text and the
6 results.

7 **Competing interests.** The authors declare that there is not any competing interest.

8 9 10 **Acknowledgements**

11
12 We acknowledge the World Climate Research Program's Working Group on Coupled Modelling, which
13 is responsible for CMIP, and we thank the climate modeling groups (listed in the Atlas GitHub) for
14 producing and making available their model output.

15 JMG and SH acknowledge support from the Spanish Government through the research and innovation
16 programme (project ref. PID2019-111481RB-I00) and the María de Maeztu excellence programme (Ref.
17 MdM-2017-0765). SHF acknowledges support from the Spanish Government through the María de
18 Maeztu excellence programme (Ref. MDM-2017-0714), and by the Basque Government through the
19 BERC 2018–2021 programme.

20 The authors are also grateful to anonymous reviewers who helped to improve the original manuscript.

21 22 **REFERENCES**

- 23
24 Balaji, V., Taylor, K. E., Juckes, M., Lawrence, B. N., Durack, P. J., Lautenschlager, M., Blanton, C.,
25 Cinquini, L., Denvil, S., Elkington, M., Guglielmo, F., Guilyardi, E., Hassell, D., Kharin, S.,
26 Kindermann, S., Nikonov, S., Radhakrishnan, A., Stockhause, M., Weigel, T., and Williams, D.:
27 Requirements for a global data infrastructure in support of CMIP6, Geoscientific Model
28 Development, 11, 3659–3680, <https://doi.org/https://doi.org/10.5194/gmd-11-3659-2018>, 2018.
- 29 Bärring, L. and Strandberg, G.: Does the projected pathway to global warming targets matter?,
30 Environmental Research Letters, 13, 024 029, <https://doi.org/10.1088/1748-9326/aa9f72>, publisher:
31 IOP Publishing, 2018.
- 32 CDO: Climate Data Operator Version 1.9.8. Max-Planck-Institute for Meteorology,
33 <https://code.mpimet.mpg.de/projects/cdo>, 2019.
- 34 CSIRO and Bureau of Meteorology 2015, Climate Change in Australia Information for Australia's Natural
35 Resource Management Regions: Technical Report, CSIRO and Bureau of Meteorology, Australia.
36 <http://www.climatechangeinaustralia.gov.au>
- 37 Christensen, J., Hewitson, B., Busuioac, A., Chen, A., Gao, X., Held, I., Jones, R., Kolli, R., Kwon, W.-T.,
38 Laprise, R., Rueda, V. M., Mearns, L., Menez, C., Rn, J., Rinke, A., Sarr, A., and Whetton, P.:
39 Climate Change 2007: The Physical Science Basis. Contribution of Working Group I to the Fourth
40 Assessment Report of the Intergovernmental Panel on Climate Change [Solomon, S., D. Qin, M.
41 Manning, Z. Chen, M. Marquis, K.B. Averyt, M. Tignor and H.L. Miller (eds.)], book section
42 Regional Climate Projections, pp. 847–940, Cambridge University Press, Cambridge, United
43 Kingdom and New York, NY, USA, 2007.
- 44 Diedhiou, A., Bichet, A., Wartenburger, R., Seneviratne, S. I., Rowell, D. P., Sylla, M. B., Diallo, I.,
45 Todzo, S., Touré, N. E., Camara, M., Ngatchah, B. N., Kane, N. A., Tall, L., and Affholder, F.:
46 Changes in climate extremes over West and Central Africa at 1.5°C and 2°C global warming,
47 Environmental Research Letters, 13, 065 020, <https://doi.org/10.1088/1748-9326/aac3e5>, 2018.
- 48 Espinoza, J.C., Ronchail, J., Marengo, J.A. et al. Contrasting North–South changes in Amazon wet-day
49 and dry-day frequency and related atmospheric features (1981–2017). Clim Dyn 52, 5413–5430,
50 2019. <https://doi.org/10.1007/s00382-018-4462-2>

1 Forster, P. M., Maycock, A. C., McKenna, C. M., and Smith, C. J.: Latest climate models confirm need
2 for urgent mitigation, *Nature Climate Change*, 10, 7–10, [https://doi.org/10.1038/s41558-019-0660-](https://doi.org/10.1038/s41558-019-0660-0)
3 0, 2020.

4 Giorgi, F. and Francisco, R.: Uncertainties in regional climate change prediction: a regional analysis of
5 ensemble simulations with the HADCM2 coupled AOGCM, *Climate Dynamics*, 16, 169–182,
6 <https://doi.org/10.1007/PL00013733>, 2000.

7 Giorgi, F., Hewitson, B., Christensen, J., Hulme, M., Storch, H. V., Whetton, P., Jones, R., Mearns, L.,
8 and Fu, C.: *Climate Change 2001: The Scientific Basis* [J. T. Houghton, Y. Ding, D. J. Griggs, M.
9 Noguera, P. J. van der Linden, X. Dai, K. Maskell, C. A. Johnson (eds.)], book section *Regional*
10 *Climate Information? Evaluation and Projections*, pp. 583–638, Cambridge University Press, 2001.

11 Harris, I. and Jones, P.: CRU TS4.03: Climatic Research Unit (CRU) Time-Series (TS) version 4.03 of
12 high-resolution gridded data of month-by-month variation in climate (Jan. 1901- Dec. 2018), Centre
13 for Environmental Data Analysis,
14 <https://doi.org/http://dx.doi.org/10.5285/10d3e3640f004c578403419aac167d82>, 2020.

15 Harris, I., Jones, P. D., Osborn, T. J., and Lister, D. H.: Updated high-resolution grids of monthly climatic
16 observations – the CRU TS3.10 Dataset, *International Journal of Climatology*, 34, 623–642,
17 <https://doi.org/10.1002/joc.3711>, 2014.

18 Hawkins, E. and Sutton, R.: The Potential to Narrow Uncertainty in Regional Climate Predictions, *Bulletin*
19 *of the American Meteorological Society*, 90, 1095–1108,
20 <https://doi.org/10.1175/2009BAMS2607.1>, 2009.

21 Hoyer, S. and Hamman, J., 2017. xarray: N-D labeled Arrays and Datasets in Python. *Journal of Open*
22 *Research Software*, 5(1), p.10. DOI: doi:10.5334/jors.148.

23 Huffman, G. J., Adler, R. F., Bolvin, D. T., and Gu, G.: Improving the global precipitation record: GPCP
24 Version 2.1, *Geophysical Research Letters*, 36, <https://doi.org/10.1029/2009GL040000>, 2009.

25 Iturbide, M., Bedia, J., Herrera, S., Baño-Medina, J., Fernández, J., Frías, M. D., Manzanar, R., San-
26 Martín, D., Cimadevilla, E., Cofiño, A. S., and Gutiérrez, J. M.: The R-based climate4R open
27 framework for reproducible climate data access and post-processing, *Environmental Modelling &*
28 *Software*, 111, 42–54, <https://doi.org/10.1016/j.envsoft.2018.09.009>, 2019.

29 Iturbide, M., Gutiérrez, J. M., Cimadevilla, E., Bedia, J., Hauser, M., and Manzanar, R.:
30 SantanderMetGroup/ATLAS GitHub (Version v1.5), <http://doi.org/10.5281/zenodo.3968318>, 2020.

31 Kotlarski, S., Szabó, P., Herrera, S., Rätty, O., Keuler, K., Soares, P. M., Cardoso, R. M., Bosshard, T.,
32 Pagé, C., Boberg, F., Gutiérrez, J. M., Isotta, F. A., Jaczewski, A., Kreienkamp, F., Liniger, M. A.,
33 Lussana, C., and Pianko-Kluczynska, K.: Observational uncertainty and regional climate model
34 evaluation: A pan-European perspective, *International Journal of Climatology*, 39, 3730–3749,
35 <https://doi.org/10.1002/joc.5249>, 2019.

36 Lange, S.: Earth2Observe, WFDEI and ERA-Interim data Merged and Bias-corrected for ISIMIP
37 (EWEMBI). V. 1.1. GFZ Data Services., <http://doi.org/10.5880/pik.2019.004>, 2019.

38 Madakumbura, G. D., Kim, H., Utsumi, N., Shiogama, H., Fischer, E. M., Seland, A., Scinocca, J. F.,
39 Mitchell, D. M., Hirabayashi, Y., and Oki, T.: Event-to-event intensification of the hydrologic cycle
40 from 1.5°C to a 2°C warmer world, *Scientific Reports*, 9, 1–7, [https://doi.org/10.1038/s41598-019-](https://doi.org/10.1038/s41598-019-39936-2)
41 39936-2, 2019.

42 Maure, G., Pinto, I., Ndebele-Murisa, M., Muthige, M., Lennard, C., Nikulin, G., Dosio, A., and Meque,
43 A.: The southern African climate under 1.5°C and 2°C of global warming as simulated by CORDEX
44 regional climate models, *Environmental Research Letters*, 13, 065 002,
45 <https://doi.org/10.1088/1748-9326/aab190>, 2018.

46 McSweeney, C. F., Jones, R. G., Lee, R. W., and Rowell, D. P.: Selecting CMIP5 GCMs for downscaling
47 over multiple regions, *Climate Dynamics*, 44, 3237–3260, [https://doi.org/10.1007/s00382-014-](https://doi.org/10.1007/s00382-014-2418-8)
48 2418-8, 2015.

49 NCC editorial: The CMIP6 landscape, *Nature Climate Change*, 9, 727–727,
50 <https://doi.org/10.1038/s41558-019-0599-1>, 2019.

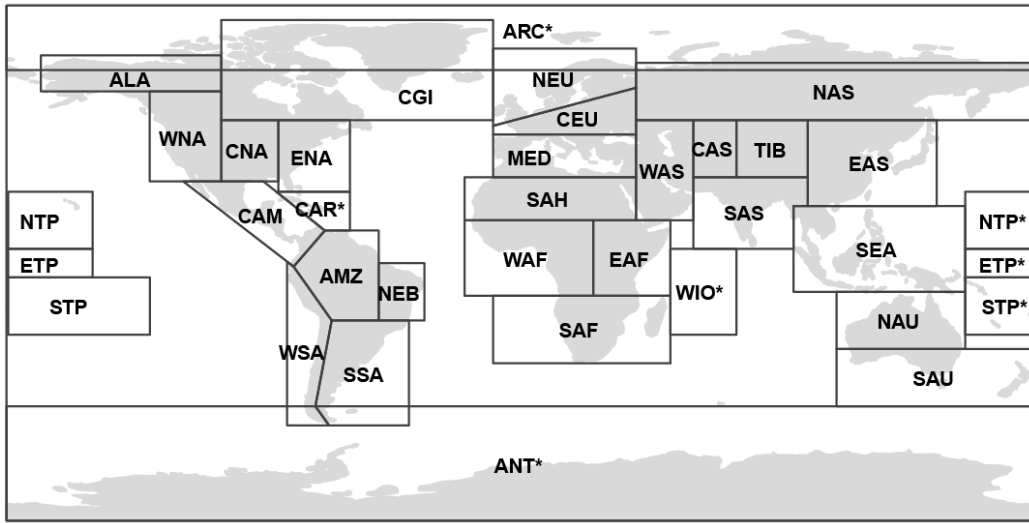
51 O’Neill, B. C., Tebaldi, C., Vuuren, D. P. v., Eyring, V., Friedlingstein, P., Hurtt, G., Knutti, R., Kriegler,
52 E., Lamarque, J.-F., Lowe, J., Meehl, G. A., Moss, R., Riahi, K., and Sanderson, B. M.: The Scenario
53 Model Intercomparison Project (ScenarioMIP) for CMIP6, *Geoscientific*
54 *Model Development*, 9, 3461–3482, <https://doi.org/https://doi.org/10.5194/gmd-9-3461-2016>, 2016.

- 1 Osima, S., Indasi, V. S., Zaroug, M., Endris, H. S., Gudoshava, M., Misiani, H. O., Nimusiima, A., Anyah,
2 R. O., Otieno, G., Ogwang, B. A., Jain, S., Kondowe, A. L., Mwangi, E., Lennard, C., Nikulin, G.,
3 and Dosio, A.: Projected climate over the Greater Horn of Africa under 1.5°C and 2°C global
4 warming, *Environmental Research Letters*, 13, 065 004, <https://doi.org/10.1088/1748-9326/aaba1b>,
5 2018.
- 6 Ruane, A. C. and McDermid, S. P.: Selection of a representative subset of global climate models that
7 captures the profile of regional changes for integrated climate impacts assessment, *Earth*
8 *Perspectives*, 4, 1, <https://doi.org/10.1186/s40322-017-0036-4>, 2017.
- 9 Rubel, F. and Kotteck, M.: Observed and projected climate shifts 1901-2100 depicted by world maps of
10 the Köppen-Geiger climate classification, *Meteorologische Zeitschrift*, pp. 135–141,
11 <https://doi.org/10.1127/0941-2948/2010/0430>, 2010.
- 12 Schneider, U., Becker, A., Finger, P., Meyer-Christoffer, A., Rudolf, B., and Ziese, M.: GPCP Full Data
13 Reanalysis Version 6.0 at 0.5: Monthly Land-Surface Precipitation from Rain-Gauges built on
14 GTS-based and Historic Data., https://doi.org/10.5676/DWD_GPCC/FD_M_V7_050, 2011.
- 15 Seneviratne, S., Nicholls, N., Easterling, D., Goodess, C., Kanae, S., Kossin, J., Luo, Y., Marengo, J.,
16 McInnes, K., Rahimi, M., Reichstein, M., Sorteberg, A., Vera, C., and Zhang, X.: Managing the
17 Risks of Extreme Events and Disasters to Advance Climate Change Adaptation [Field, Barros,
18 Stocker et al. (eds.)], book section Changes in climate extremes and their impacts on the natural
19 physical environment, pp. 109–230, Cambridge University Press, Cambridge, United Kingdom and
20 New York, NY, USA, 2012.
- 21 Sun, Q., Miao, C., Duan, Q., Ashouri, H., Sorooshian, S., and Hsu, K.-L.: A Review of Global
22 Precipitation Data Sets: Data Sources, Estimation, and Intercomparisons, *Reviews of Geophysics*,
23 56, 79–107, <https://doi.org/10.1002/2017RG000574>, 2018.
- 24 Taylor, K. E., Stouffer, R. J., and Meehl, G. A.: An Overview of CMIP5 and the Experiment Design,
25 *Bulletin of the American Meteorological Society*, 93, 485–498, [https://doi.org/10.1175/BAMS-D-](https://doi.org/10.1175/BAMS-D-11-00094.1)
26 11-00094.1, 2012.
- 27 van Oldenborgh, G.J., M. C., Arblaster, J., Christensen, J., Marotzke, J., Power, S., Rummukainen, M.,
28 and Zhou, T.: Climate Change 2013: The Physical Science Basis. Contribution of Working Group I
29 to the Fifth Assessment Report of the Intergovernmental Panel on Climate Change [Stocker, T.F.
30 and Qin, D. and Plattner, G.-K. and Tignor, M. and Allen, S.K. and Boschung, J. and Nauels, A. and
31 Xia, Y. and Bex, V. and Midgley, P.M. (eds.)], book section Annex I: Atlas of Global and Regional
32 Climate Projections, pp. 1311–1394, Cambridge University Press, Cambridge, United Kingdom and
33 New York, NY, USA, <https://doi.org/10.1017/CBO9781107415324.029>,
34 www.climatechange2013.org, 2013.
- 35
- 36 WMO: WMO Guidelines on the Calculation of Climate Normals. WMO - No. 1203,
37 https://library.wmo.int/doc_num.php?explnum_id=4166, 2017.
- 38
39
40
41
42
43
44
45
46
47
48
49
50
51
52
53

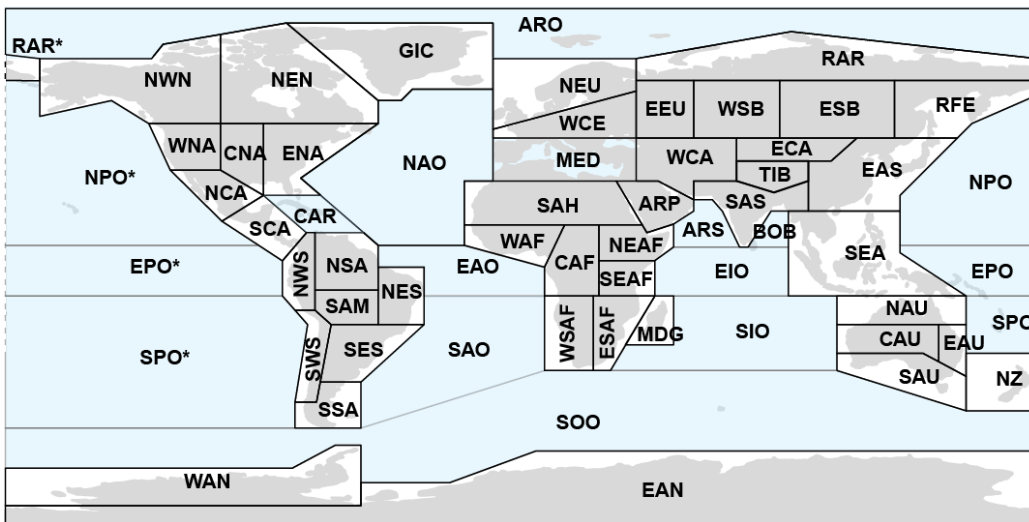
1
2
3

FIGURES

(a) IPCC AR5-WGI Reference Regions



(b) Updated Reference Regions

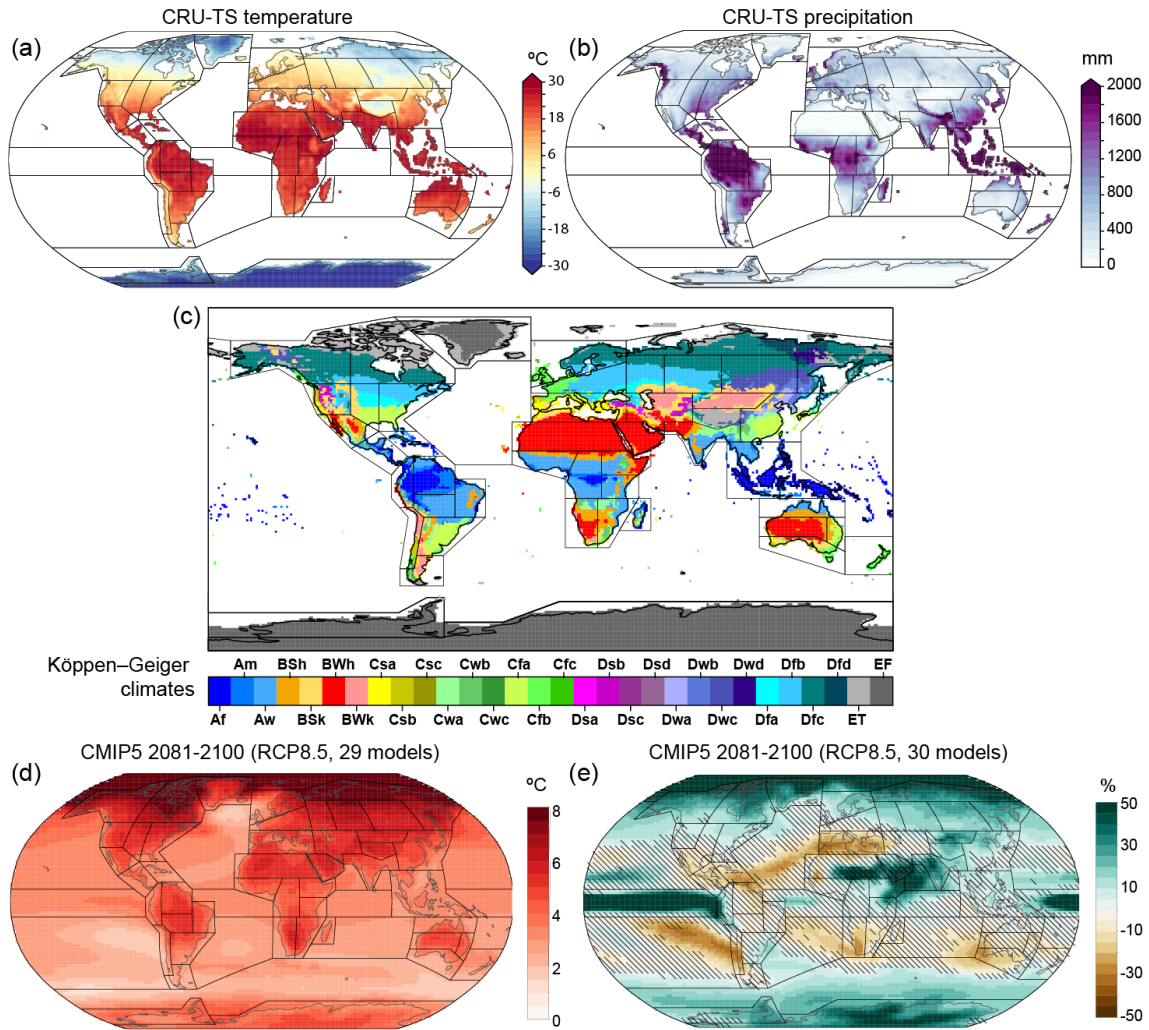


1	GIC	Greenland/Iceland	21	SAH	Sahara	40	NAU	N.Australia
2	NWN	N.W.North-America	22	WAF	Western-Africa	41	CAU	C.Australia
3	NEN	N.E.North-America	23	CAF	Central-Africa	42	EAU	E.Australia
4	WNA	W.North-America	24	NEAF	N.Eastern-Africa	43	SAU	S.Australia
5	CNA	C.North-America	25	SEAF	S.Eastern-Africa	44	NZ	New-Zealand
6	ENA	E.North-America	26	WSAF	W.Southern-Africa	45	EAN	E.Antarctica
7	NCA	N.Central-America	27	ESAF	E.Southern-Africa	46	WAN	W.Antarctica
8	SCA	S.Central-America	28	MDG	Madagascar	47	ARO	Arctic-Ocean
9	CAR	Caribbean	29	RAR	Russian-Arctic	48	NPO	N.Pacific-Ocean
10	NWS	N.W.South-America	30	WSB	W.Siberia	49	EPO	Equatorial.Pacific-Ocean
11	NSA	N.South-America	31	ESB	E.Siberia	50	SPO	S.Pacific-Ocean
12	NES	N.E.South-America	32	RFE	Russian-Far-East	51	NAO	N.Atlantic-Ocean
13	SAM	South-American-Monsoon	33	WCA	W.C.Asia	52	EAO	Equatorial.Atlantic-Ocean
14	SWS	S.W.South-America	34	ECA	E.C.Asia	53	SAO	S.Atlantic-Ocean
15	SES	S.E.South-America	35	TIB	Tibetan-Plateau	54	ARS	Arabian-Sea
16	SSA	S.South-America	36	EAS	E.Asia	55	BOB	Bay-of-Bengal
17	NEU	N.Europe	37	ARP	Arabian-Peninsula	56	EIO	Equatorial.Indic-Ocean
18	WCE	Western&Central-Europe	38	SAS	S.Asia	57	SIO	S.Indic-Ocean
19	EEU	E.Europe	39	SEA	S.E.Asia	58	SOO	Southern-Ocean
20	MED	Mediterranean						

4
5
6
7
8
9

Figure 1. Updated IPCC reference land (gray shading) and ocean (blue shading) regions; note that the Caribbean and the Meditterean are considered both land and ocean regions (defined using the land and sea masks, respectively). Land masks are used to obtain land-only information for land regions (excluding the coastal white regions).

1



2

3

4

5

6

7

8

9

10

11

12

13

14

15

16

17

18

19

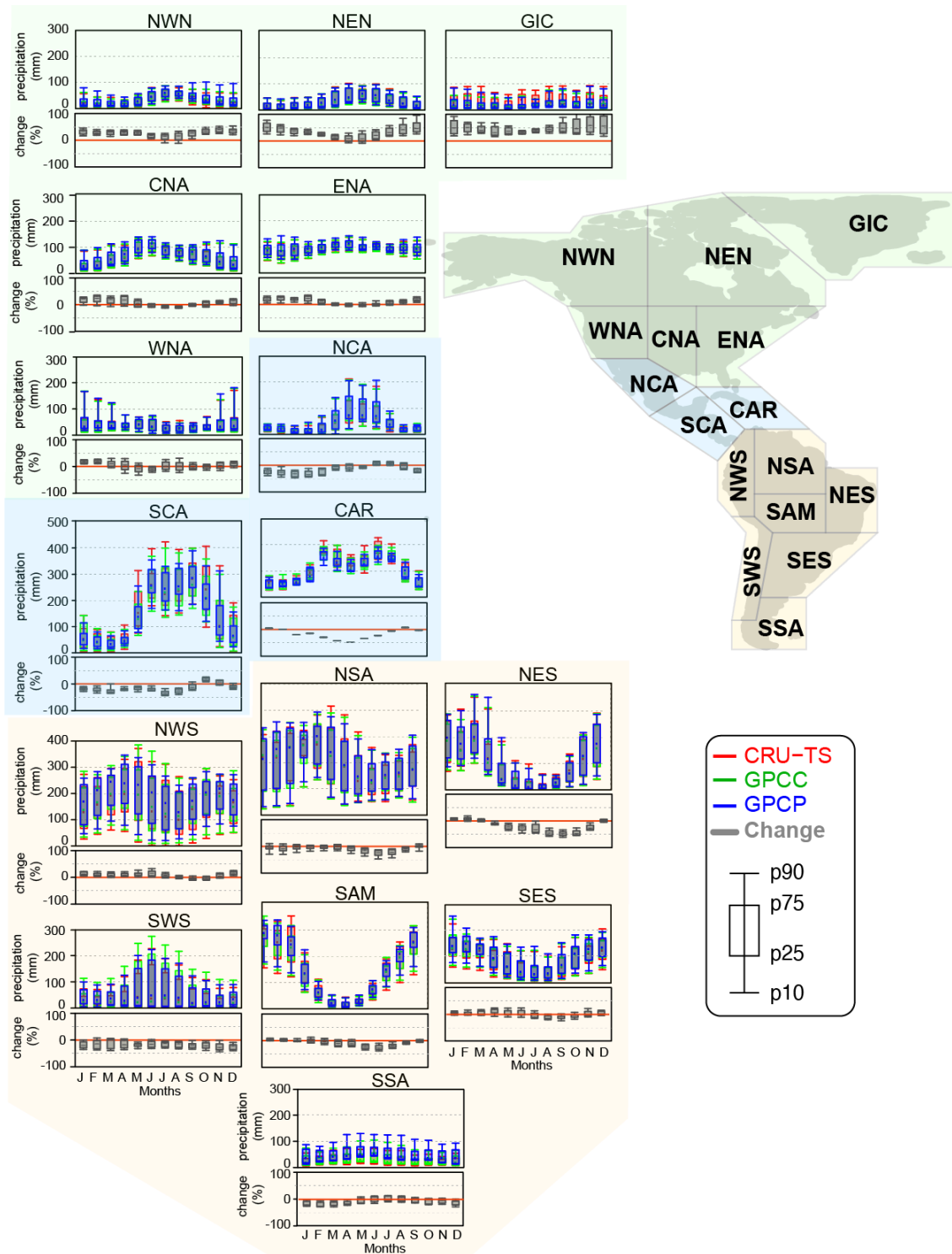
20

21

22

23

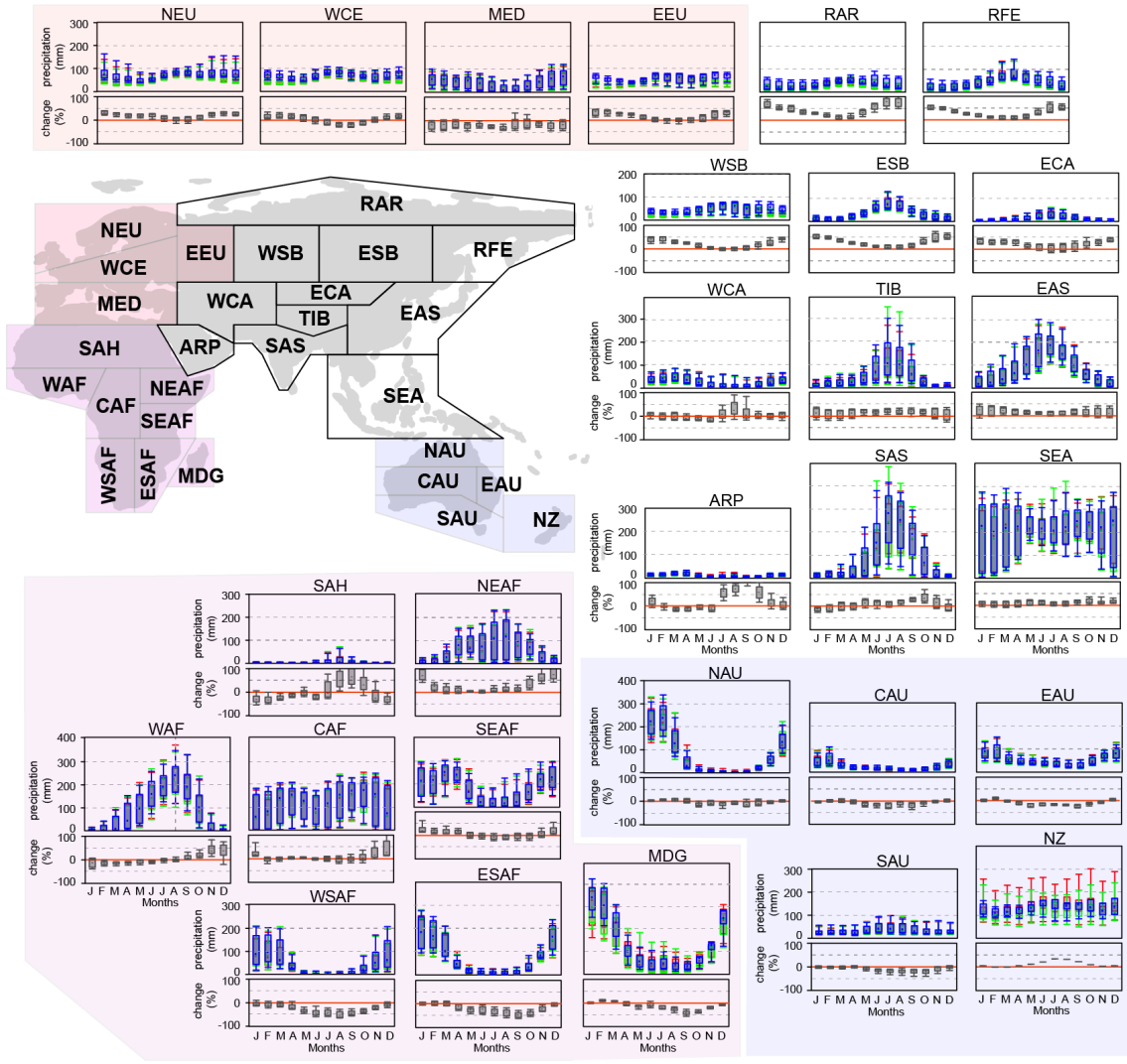
Figure 2. (a) Global mean temperature, (b) accumulated precipitation and (c) Köppen-Geiger climate classification from the CRU-TS dataset for the period 1981-2010 (data for Antarctica is filled with the EWEMBI dataset). This information is used to characterize the regional climate consistency of the reference regions (solid lines). (d,e) Climate change projections for temperature and precipitation, respectively, from the CMIP5 curated dataset for RCP8.5 2081-2100 w.r.t. the AR5 modern climate baseline 1986-2005. Hatching indicates weak (less than 80%) model agreement on the sign of the change.



1
2
3
4
5
6
7
8
9
10

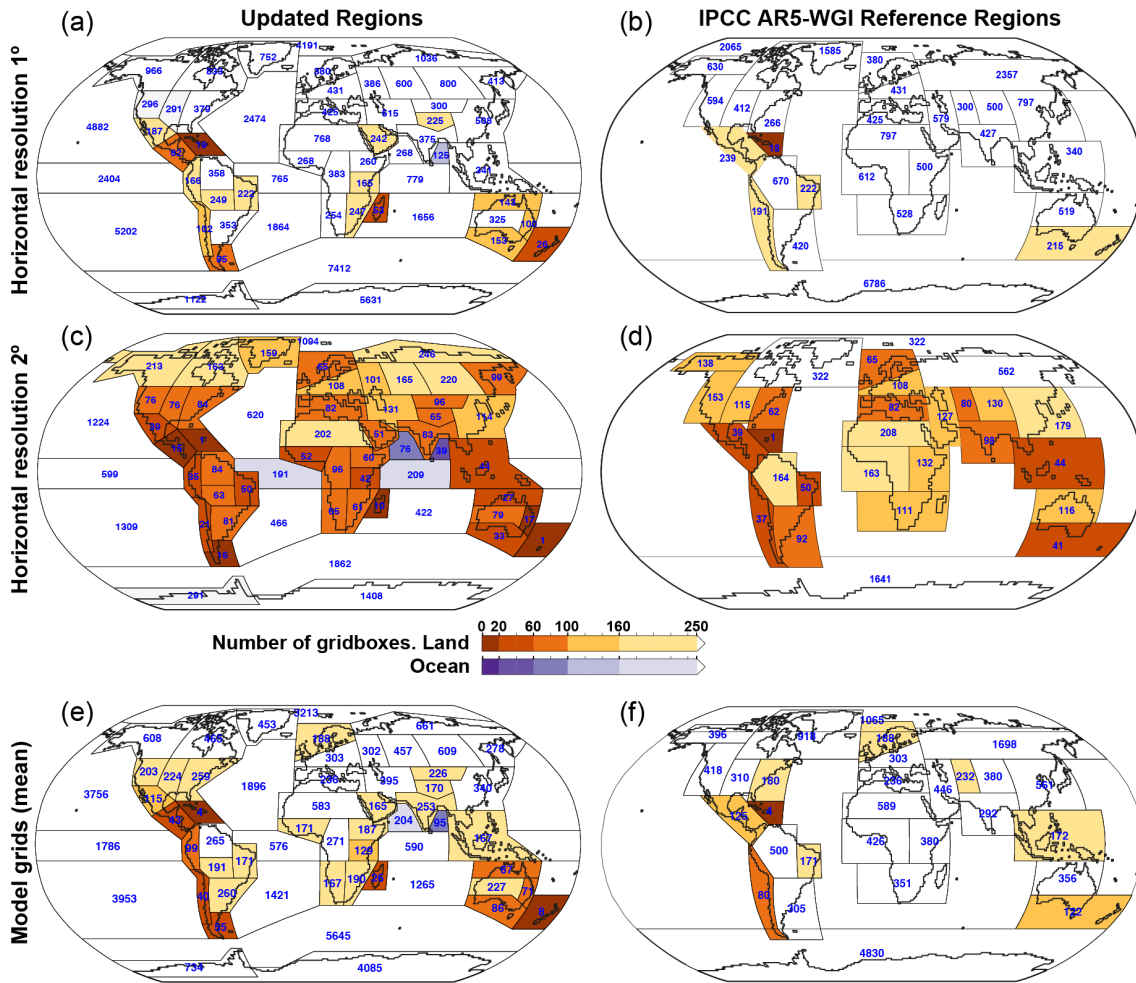
Figure 3. Observed annual cycle (1981-2010) for precipitation for the American reference regions from three different observational datasets (CRU-TS, GPCC, GPCP) and climate change signal (RCP8.5, 2081-2100 w.r.t. the AR5 modern climate baseline 1986-2005). The panel for each reference region shows the observed annual cycle (top, in monthly accumulated mm) and the monthly projected changes (bottom, in gray, as %); box and whiskers plots represent the spatial (gridbox) spread of monthly values over the region.

1
2
3



5
6
7
8
9
10
11
12

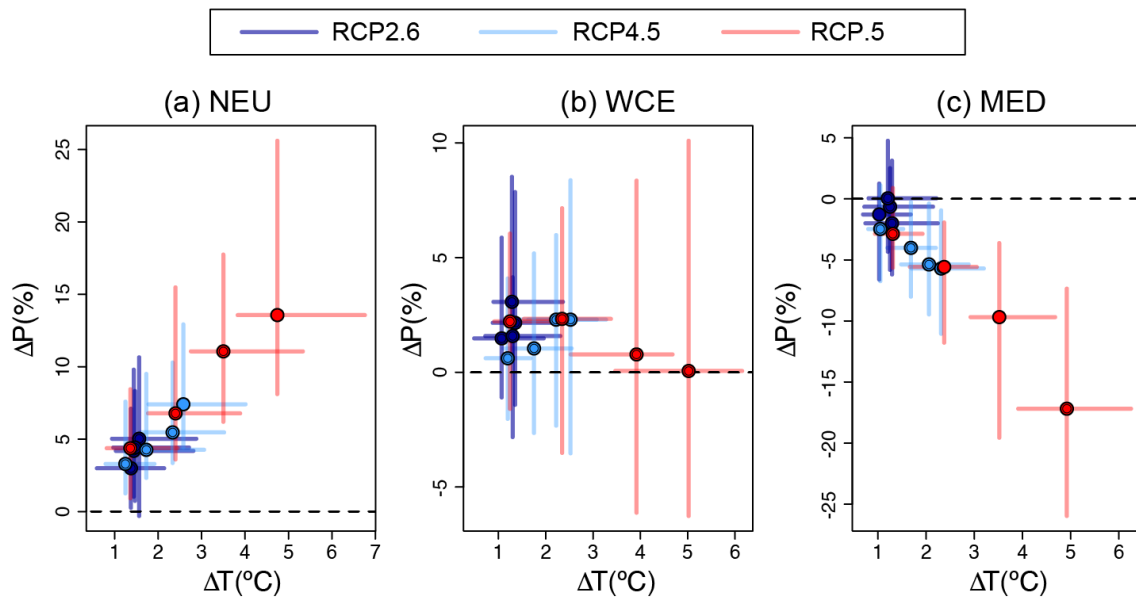
Figure 4. As figure 3 but for Europe, Asia and Australasia.



1
2
3
4
5
6
7
8

Figure 5. Number of gridboxes encompassed by the different reference regions for 1° (a,b) and 2° (c,d) resolution and for the CMIP6 model grids (e,f) –the multi-model mean is represented–, considering the updated (a,c,e) and the original AR5 (b,d,f) reference regions. Colors indicate regions with less than 250 gridboxes. The blue numbers in each of the regions show the number of gridboxes (only land gridboxes for land regions).

1
2
3
4



5
6
7
8
9
10
11
12
13
14
15
16
17
18

Figure 6. Illustrative example of the use of reference regions and aggregated CMIP5 datasets: Regional mean changes in annual mean temperature and precipitation for three European regions (NEU, WCE and MED) for four future periods (2021-2040, 2041-2060, 2061-2080, 2081-2100), as obtained from CMIP5 projections. Changes are absolute for temperature and relative for precipitation. Horizontal and vertical error bars represent ± 1 standard deviation from the mean calculated across the ensemble of included models. The script to generate this figure for all the 55 land and ocean regions (including the global region) from the ready-to-use aggregated CMIP5 datasets is available at the ATLAS GitHub, and can be adapted to produce similar results for alternative datasets (e.g. CMIP6).